Targeting Type IV pili as an antivirulence strategy against invasive meningococcal disease

Kevin Denis, Marion Le Bris, Loïc Le Guennec, Jean-Philippe Barnier, Camille Faure, Anne Gouge, Haniaa Bouzinba-Ségard, Anne Jamet, Daniel Euphrasie, Beatrice Durel, et al.

Targeting Type IV pili as an antivirulence strategy against invasive meningococcal disease

Kevin Denis[1,2,3], Marion Le Bris[1,2,3], Loic le Guennec[1,2,3], Jean-Philippe Barnier[4,5,6,7], Camille Faure[1,2,3], Anne Gouge[1,2,3], Haniaa Bouzinba-Ségard[1,2,3], Anne Jamet[4,5,6,7], Daniel Euphrasie[4,5,6,7], Beatrice Durel[1,2,3], Nicolas Barois[8,9,10,11], Philippe Pelissier[12], Philippe C. Morand[1,2,3], Mathieu Coureuil[4,5,6], Frank Lafont[8,9,10,11], Olivier Join-Lambert[4,5,6,7] Xavier Nassif [4,5,6,7] and Sandrine Bourdoulous[1,2,3,*]

[1] Inserm, U1016, Institut Cochin, Paris, France
[2] CNRS, UMR8104, Paris, France
[3] Université Paris Descartes, Sorbonne Paris Cité, France.
[4] Inserm, unité U1151, Institut-Necker-Enfants-Malades, Paris, France
[5] CNRS, UMR 8253, Paris, France
[6] Université Paris Descartes, Sorbonne Paris Cité, Faculté de médecine, Paris, France
[7] Assistance Publique – Hôpitaux de Paris, Hôpital Necker Enfants Malades, Paris, France
[8] Cellular Microbiology and Physics of infection group, Center for Infection and Immunity of Lille, Institut Pasteur de Lille, 59000 Lille, France
[9] CNRS UMR 8204, 59000 Lille, France
[10] INSERM U1019, 59000 Lille, France,
[11] Université de Lille, 59000 Lille, France
[12] Service de Chirurgie Reconstructrice et Plastique, Fondation Hôpital Saint Joseph, Paris, France

* To whom correspondence should be addressed. E-mail: sandrine.bourdoulous@inserm.fr

Bacterial virulence factors are attractive targets for therapeutics development. Type IV pili, which are associated with a remarkable array of properties ranging from motility to the interaction between bacteria and attachment to biotic and abiotic surfaces, represent particularly appealing virulence factor targets. Type IV pili are present in numerous bacterial species and are critical for their pathogenesis. In this study, we report that Trifluoperazine and related phenothiazines block functions associated with type IV pili in different bacterial pathogens, by affecting piliation within minutes. Using *Neisseria meningitidis* as a paradigm of Gram-negative bacterial pathogens requiring type IV pili for pathogenesis, we show that piliation was sensitive to altered Na+ pumping activity of Na^+-NQR complex and that these compounds most likely altered the establishment of the sodium gradient. *In vivo*, these compounds exert a strong protective effect. They reduce meningococcal colonization of the human vessels, prevent subsequent vascular dysfunctions, intravascular coagulation and overwhelming inflammation, the hallmarks of invasive meningococcal infections. Finally, they reduce lethality. This work provides proof of concept that compounds with activity against bacterial type IV pili could beneficially participate in the treatment of infections caused by type IV pilus-expressing bacteria.

INTRODUCTION

Type IV pili, produced by numerous pathogenic bacteria, are filamentous bacterial appendages present in both Gram-negative and Gram-positive bacteria[1]. These attributes mediate an extraordinary array of functions, including motility, DNA uptake, bacterial aggregation or adherence to abiotic surface or host cells, and are essential in bacterial pathogenesis[2]. They are made of the assembly of pilin subunits into a long helical structure, translocated through a pore in the outer membrane. Most type IV pili are highly dynamic, as they can rapidly retract and elongate, a process enabling twitching motility[3,4]. Their dynamic extension/retraction cycle centers on two cytoplasmic ATPases with antagonistic functions, highly conserved among the very widespread bacteria with retractable pili, implicating a fundamentally conserved mechanism of type IV pilus biology[1]. Due to their prominent display on the surfaces of many bacterial pathogens and their vital role in virulence, type IV pilus structures are particularly attractive targets for the design of therapies.

In pathogenic *Neisseria meningitidis* (meningococcus), type IV pili are key virulence factors. They are made of the assembly of pilus subunits (PilE) and of other less abundant "minor" pilins that play an important role in fine-tuning type IV pilus function[5-7]. Meningococci, which normally reside asymptomatically on the human nasopharyngeal mucosa, are pathogenic when they gain access to the bloodstream as they can provoke two devastating diseases, *purpura fulminans* and meningitis, rapidly causing death or permanent disability, despite prompt antibiotics treatments[8]. Circulating meningococci adhere to the endothelium lining microvessels through a direct binding of type IV pili with endothelial receptor complexes[9-11]. Bacteria then rapidly proliferate, forming aggregated bacterial colonies at the endothelial cell surface, and promote signaling events that contribute to vascular alterations[9,12]. Colonization of brain microvessels is a prerequisite to cross the blood-brain barrier, allowing bacteria to reach the meninges where they multiply, causing meningitis, whereas, skin lesions occur secondary to meningococcal colonization of dermal vessels, which can eventually lead to *purpura fulminans*[13]. Skin lesion extension correlates with irreversible endothelial ischaemic injury with extravasation of blood cells into the dermis and necrosis. Circulating bacteria elicit systemic inflammation characterized by massive activation of both macrophages in the reticuloendothelial system and circulating leukocytes. Through the synthesis and secretion of pro-inflammatory cytokines, endothelial cells also contribute to both local and systemic inflammation, resulting in septic shock and multiple organ failure[14,15]. High levels of inflammatory cytokines including Interleukin-6 (IL-6), IL-8 and TNFα in patient serum closely correlate with the clinical severity of the disease[16,17]. Importantly, type IV pilus-dependent adhesion of meningococci to human microvasculature is determinant to the triggering of both vascular purpuric lesions and

inflammation[15,18], and a prerequisite to sustained bacteremia responsible for sepsis and subsequent lethality[19].

Here, we demonstrate that trifluoperazine and related phenothiazines, a family of compounds previously used in human medicine to treat psychotic disorders, block the functions carried by type IV pili in different bacterial pathogens, by inducing pilus retraction within minutes. Using *N. meningitidis* as a model organism, we show that these compounds regulate piliation most likely by acting on the Na^+-NQR complex, which drives the selective translocation of Na^+ across the inner membrane, thereby building a sodium motive force. We further showed that establishment of a sodium gradient is required for piliation**.** *In vivo,* these compounds suppress the consequences of type IV pilus-dependent pathogenesis, thus opening a new era for the treatment of infections due to type IV pilus-expressing bacteria.

RESULTS

Trifluoperazine blocks the functions carried by bacterial type IV pili

When grown in broth for two hours, meningococci form bacterial aggregates due to interbacterial interactions, a phenotype carried by type IV pili in capsulated bacteria[1,5]. We fortuitously observed that trifluoperazine, initially used *in vitro* as a calmodulin antagonist, rapidly induced the dispersion of bacterial aggregates (Fig. 1a). This effect was dose-dependent (Fig. 1a and 1b), and it occurred within minutes (Fig. 1c and Video 1). Trifluoperazine first induced a reduction in bacterial twitching motility, shortly followed by the dispersal of the bacterial aggregates (Fig. 1d and Video 2). In contrast to trifluoperazine treatment, addition of bactericidal antibiotics used in the treatment of meningococcaemia, such as third generation cephalosporin cefotaxime or aminoglycoside gentamicin, poorly affected aggregation (Fig. 1a). Although trifluoperazine showed some antimicrobial activity against *N. meningitidis*, this was observed at later time point (24h after treatment) and was not as efficient as antibiotics (Supplementary Fig. 1a). Furthermore, treatment with trifluoperazine poorly affected bacterial growth during the first hour of treatment (Supplementary Fig. 1b) while it rapidly and reversibly dispersed bacterial aggregates (Supplementary Fig. 2).

The dispersal effect of trifluoperazine was observed with meningococcal strains belonging to different sequence types and to different capsular serogroups (Supplementary Fig. 3a). Trifluoperazine was also able to reduce twitching motility and aggregates of strains of the related species, *Neisseria gonorrhoeae*, which causes gonorrhea (Supplementary Fig. 3B and Video 3). This effect was not limited to *Neisseria* species, as treatment with trifluoperazine also reduced by 40 % the pilus-dependent twitching motility of the opportunistic pathogen *Pseudomonas aeruginosa PAO1*, whereas it did not affect its swarming behaviour, which requires functional flagella (Supplementary Fig. 4a). Furthermore, trifluoperazine also induced bacterial dispersion from *PAO*1 biofilms, as shown by the loss of the 3D community (Supplementary Fig. 4b).

Trifluoperazine belongs to a large family of phenothiazine derivatives belonging to three groups: the aliphatic compounds, the piperidines and the piperazines (Supplementary Table 1). All piperazine and piperidine compounds tested induced the dispersal of liquid-grown meningococcal aggregates, in a dose-dependent manner, but with varying efficiency (Supplementary Fig. 5). By contrast, no effect was observed with the aliphatic compounds in this range of concentrations excepted for promazine. Thioridazine was the most effective compound *in vitro*, promoting the dispersal of bacterial aggregation at concentrations 10-fold lower than trifluoperazine, without bactericidal effect (Supplementary Fig. 6).

These data demonstrate that trifluoperazine and related phenothiazines induced the dispersal of meningococcal aggregates by a mechanism independent from bactericidal activity.

Phenothiazines regulate the piliation status of meningococci

We then examined the effect of trifluoperazine and thioridazine on the piliation status of meningococci. Wild type (WT) meningococci treated with cefotaxime or gentamicin for 30 minutes expressed type IV pili on their surface similarly to non-treated bacteria (Supplementary Fig. 7a). Conversely, few type IV pili were observed on bacteria treated for 30 min with trifluoperazine or thioridazine (Fig. 2a), suggesting that these compounds induced fiber dissociation or retraction. Interestingly, trifluoperazine and thioridazine did not affect aggregation on a retraction–defective PilT-deleted mutant (ΔPilT) (Fig. 1c, Video 4 and Supplementary Fig. 7b), and it did not affect type IV pilus surface expression in the ΔPilT mutant (Fig. 2a and Supplementary Fig. 7c). Consistently, trifluoperazine did not significantly affect expression levels of the major pilin subunit PilE, nor of the ATPase PilT (Supplementary Fig. 7d). However, in contrast to non-treated bacteria that form large bundles of type IV pili at the bacterial surface, trifluoperazine treatment induced the enrichment of PilE within the bacterial body, most likely in the inner membrane that is the reservoir for pilin subunits[1] (Fig. 2b).

The above results strongly suggested that trifluoperazine favoured pilus retraction over pilus biogenesis. To confirm this hypothesis, we monitored bacterial liquid growth in the presence of trifluoperazine. This treatment inhibited the formation of aggregates by wild type bacteria, whereas it poorly affected aggregation of the PilT mutant strain (Supplementary Fig. 8), thus ruling out a possible effect on pilus biogenesis. Besides PilT, the outer membrane proteins PilC also play a major role in controlling pilus retraction by antagonising pilus retraction[20]. To address whether antagonizing pilus retraction would provide resistance to the effect of trifluoperazine, we used a strain overexpressing PilC1 (*PilC1*ind). Similarly to the ΔPilT mutant, trifluoperazine did not affect the inducible aggregation of a *PilC1*ind strain (Supplementary Fig 7e), nor did it regulate the expression level of PilC1 (Supplementary Fig. 7d). These results demonstrated that trifluoperazine interferes with pilus dynamics.

To characterize the mechanisms by which these compounds affected meningococcal piliation, we generated strains resistant to the bactericidal activity of trifluoperazine. Four clones were forming bacterial aggregates in suspension and were resistant to the dispersal effect of both trifluoperazine and thioridazine (Supplementary Fig. 9). All clones had genetic alterations in one of 6 genes encoding for the sodium pumping NADH:ubiquinone oxidoreductase complex (Na^+-NqrA-F) (Supplementary Table 2), which is crucial for establishing an electrochemical Na^+ gradient across the

inner membrane[21]. In addition, all clones had alterations in genes encoding either the glycosyltransferase lgtE or the UDP-glucose 4-epimerase GalE, both essential for incorporation of galactose into meningococcal lipopolysaccharide (LOS). Changes in LOS structure is a previously reported adaptive mechanism to osmotic pressure[22,23], suggesting that mutations affecting LOS structure might compensate for alterations in Na^+ transport due to mutations in Nqr subunits. Interestingly, meningococcal isogenic *ΔNqrA-F* mutants, devoid of individual *nqr* genes and with wild type GalE, were poorly piliated and aggregative (Fig. 2c), thus linking piliation and Nqr-mediated Na^+ pumping activity. We therefore hypothesized that trifluoperazine and thioridazine might affect sodium gradient through the inner membrane. Enrichment of broth with NaCl from 6,4 g/L (close to blood sodium level) to 21,4 g/L did not affect the aggregation for the WT meningococci (Fig. 2D). However, NaCl inhibited the dispersal effect of both trifluoperazine and thioridazine, in a dose-dependent manner. This effect was specific of the Na^+ ions and independent from an osmotic stress, as addition of KCl up to 22,4 g/L had no inhibitory effect (Fig. 2D). Altogether, these results strongly suggested that trifluoperazine and thioridazine rapidly affect piliation by altering the Na^+ pumping activity of Na^+-NQR.

Phenothiazines reduce bacteria-induced endothelial cell injury *in vitro*

Next, we analysed the effect of these phenothiazines on initial adhesion to human endothelial cells and microcolony formation, as both rely on expression of type IV pili. When pre-treated with trifluoperazine, bacteria poorly adhered and/or formed bacterial colony at the surface of primary human endothelial cells isolated from dermal microvessels HDMECs (Supplementary Fig. 10). More interestingly, when applied to meningococcal microcolonies already established at endothelial cell surface, trifluoperazine or thioridiazine treatment for 30 min disrupted the preformed microcolonies, thus allowing the release of adherent bacteria. This effect was dose-dependent and was observed on human endothelial cells isolated from microvessels, either form dermis (HDMEC) (Fig. 3a and 3b) or from brain (hCMEC/D3) (Supplementary Fig. 11). The effect of both phenothiazines was further confirmed by scanning electron microscopy analysis. Whereas bacteria formed large 3D colonies in control conditions, only few and dispersed bacteria remained at the endothelial cell surface after treatment (Fig. 3d). As expected, the two phenothiazines did not induce the dispersal of microcolonies formed on endothelial cells by the *ΔPilT* mutant (Fig. 3a and 3c). In contrast to phenothiazines, addition of gentamicin or cefotaxime poorly induced the dispersal of microcolonies formed by wild type meningococci (Fig. 3a and 3b).

We further analyzed the effect of trifluoperazine on the colonization of human brain vessels, using an *ex vivo* meningococcal infection model of fresh human frontal brain tissues, as described

previously[10]. Upon infection, meningococci replicated as microcolonies adjacent to VE-cadherin-positive endothelial cells (Fig. 3e). Consistent with *in vitro* cellular models, treatment of infected brain sections with trifluoperazine for 30 min induced the dispersal of meningococcal microcolonies, reducing by 80% the vascular colonization of the human brain vessels (Fig. 3e and 3f).

Blood flow playing a pivotal role in stabilizing barrier function[24], we then addressed the impact of these phenothiazines on endothelial cell dysfunctions promoted by adherent bacteria, using HDMECs grown under laminar shear stress. As previously observed, control conditions showed meningococci-induced dismantlement of the continuous VE-cadherin staining at the endothelial cell junctions, as well asformation of gaps between cells (Fig. 4a). Cefotaxime, although reducing bacterial colonization, had no protective effect on vascular cell junction integrity. In contrast, trifluoperazine, alone or in combination with cefotaxime, induced the dispersion of most bacterial colonies and restored VE-cadherin continuity at intercellular junctions (Fig. 4a). Hence, in contrast to antibiotic treatment, trifluoperazine rapidly prevents the deleterious signalling events leading to altered cell junction integrity.

To assess a potential protective effect of phenothiazines on basement membrane integrity, HDMECs were grown on a fluorescent gelatin matrix (Gelatin-FITC) (Fig. 4b). In the absence of infection, <5% of the basement membrane was degraded. Because it takes 16 to 24h to observe matrix degradation, the time for proteinases expression, bactericidal treatment was applied after 5 hours of infection to avoid bacterial overload and subsequent artefactual cell death. In these conditions, degradation of the basement membrane induced by meningococcal infection, observed 24h post-infection, was reduced in a dose-dependent manner (40 to 50 %) upon treatment with trifluoperazine or thioridazine (Fig. 4b-d). Altogether, these results demonstrated that trifluoperazine and thioridazine induce a cytoprotective effect on endothelial cells, by preserving the integrity of their endothelial cell junctions and basement membrane.

Phenothiazines reduce bacterial colonization of human blood vessels *in vivo*

We investigated the potential effect of phenothiazines on endothelial colonization by meningococci *in vivo*, using a validated humanized mouse model of meningococcal infection using severe combined immunodeficiency (SCID) mice grafted with human skin[10,15,18]. To mimic the conditions in patients with meningococcemia, grafted mice were infected with $5x10^6$ bacteria intravenously, leading to an average bacteremia of $5x10^5$ to 10^6 bacteria/ml 1h post-infection (Supplementary Fig. 12). Two hrs post-infection, bacteria had already adhered to human skin graft blood vessels; occasionally, bacterial aggregates filled the entire vessel and platelet aggregation was observed in close proximity of bacteria. Four hrs post-infection, bacteria massively colonized the human dermal vasculature with massive platelet aggregation and the integrity of the basement membrane was altered, as assessed

by staining of collagen IV, a major basement membrane constituent (Supplementary Fig. 12). To address the effect of the two phenothiazines *in vivo*, the compounds were administrated intraperitoneally 2 hours after infection and mice were sacrificed 4h post-infection (Fig. 5a). Whereas bacteremia was similar in control and treated mice (Fig. 5b), meningococcal vascular colonization was reduced by 50 to 55 % in the presence of trifluoperazine (40 mg/kg) or thioridazine (4 mg/kg), whith both number of colonized vessels and extent of bacterial colonization being decreased (Fig. 5c-d). The effect of trifluoperazine was stronger when administrated at 40 mg/kg than 24 mg/kg, or at 30 min post-infection compared to 2h, indicating that early treatment improved efficacy (Supplementary Fig. 13a-f). These results demonstrated the potent action of these two phenothiazines on vascular colonization by meningococci *in vivo*.

Phenothiazines reduce the formation of vascular lesions

We therefore examined whether reduced meningococcal colonization of the human vessels promoted by phenothiazines could prevent vascular dysfunction. First, we observed decreased platelet and red blood cell aggregation in skin grafts of phenothiazine-treated mice (Fig. 5c and 5e). This effect was dose-dependent (Supplementary Fig. 13c and 13f). In contrast to infected control grafts, in which massively colonized human dermal vessels presented signs of compromised endothelial integrity, phenothiazine treatment preserved the integrity of the endothelial cell junctions, as assessed by the continuous staining of two adherens junction markers, PECAM-1/CD31 and VE-cadherin (Fig. 5c and supplementary Fig. 13c). Second, trifluoperazine reduced by 50 to 80% the transcription of several human inflammatory cytokines induced by infection, such as IL-6, CXCL8/IL-8, CXCL1/GROα or CCL2/MCP-1 or of prostaglandin G/H synthase (PTGS2/Cox2) responsible for production of inflammatory prostaglandins (Supplementary Fig. 13g). Finally, whereas infection induced the release of TNFα, IL-6 and IL-8 in mice sera, either trifluoperazine or thioridazine treatment reduced by 45 to 60% the serum level of these pro-inflammatory factors (Fig. 5f). These data demonstrated that, by decreasing vascular colonization, phenothiazines reduce vascular alteration, thrombosis and inflammation during meningococcemia.

Thioridazine improves the outcome of meningococcal infection

We therefore addressed whether vessel clearance by thioridazine improved the outcome of infected mice (Fig. 6a). In control mice, infection with 10^6 bacteria intravenously led to an average bacteremia of $5x10^6$ bacteria/ml at 4h post-infection. Bacteremia was sustained at an average of 10^6 to $5x10^6$ bacteria/ml at 18h and 48h post-infection and 85 % of the infected control mice did not survive by day 2 (Fig. 6b and 6c). Upon treatment with thioridazine 2h after infection, while the bacteremia was

267 similar to that of control mice at 4h post-infection, it was reduced down to $5x10^3$ to $5x10^4$
268 bacteria/ml at 18h and eventually dropped to $<10^2$ bacteria/ml at 48h post-infection (Fig. 6b). 0nly
269 40% of the thioridazine-treated mice died 48h post-infection (Fig. 6c). As observed at 4h post-
270 infection, in contrast to infected control grafts in which human dermal vessels were massively
271 colonized, thrombosed and presented signs of compromised endothelial integrity at time of death
272 (between 18h and 48h post-infection), thioridazine had largely reduced colonization and subsequent
273 signs of thrombosis and preserved vascular integrity at 72h post-infection (Fig. 6d). These data
274 demonstrated the improvement of survival outcome with the use of thioridazine in an *in vivo* model
275 of meningococcal infection.
276
277 **Thioridazine has adjunctive effects over antibiotic treatment**
278 Since antibiotics are a key element for medical treatment of meningococcemia, we analysed whether
279 thioridazine could provide a beneficial effect when administrated with antibiotics. When applied 2h
280 post-infection at doses recommended for patients with suspected acute bacterial meningitis (200
281 mg/kg/day), cefotaxime exerted a strong bactericidal effect as bacteremia dropped to less than 10^2
282 bacteria/ml at 4h post-infection (Fig. 6a and 6b) and as it totally prevented mice lethality (Fig. 6c). It
283 reduced by 90 % vascular colonization by meningococci (Fig. 6e and 6f). However, thrombosis (Fig. 6E
284 and 6F) was increased in cefotaxime-treated mice and serum concentration of human inflammatory
285 cytokines TNFα, IL-6 and IL-8 were not significantly reduce 4h post-infection (Fig. 6g). When
286 administrated with cefotaxime, thioridazine reduced by 70% the signs of thrombosis (Fig. 6e and 6f)
287 and reduced vascular inflammation (Fig. 6g). 72h post-infection, whereas cefotaxime-treated grafts
288 still presented signs of vascular alterations and thrombosis, associated with massive infiltration of
289 polymorphonuclear neutrophils, these effects were prevented by the addition of thioridazine (Fig.
290 6d), therefore demonstrating that thioridazine had adjunctive effects over antibiotic treatment by
291 reducing alteration of blood vessels and the overwhelming inflammatory response.
292
293 Collectively, these results demonstrate that targeting type IV pili, a major meningococcal
294 virulence factor, with some phenothiazines exert a protective effect on the pathophysiological events
295 of meningococcemia. Their use in combination with antibiotics may reduce incidence of vascular
296 alteration, intravascular coagulation and inflammatory disorders in meningococcal diseases.
297
298

DISCUSSION

Much investigation has been conducted in recent years to improve treatments of infectious diseases, especially in the light of incomplete action, adverse effects, and increasing resistance to antibiotics. This implies the development of pharmaceuticals acting on previously unutilized conserved targets[25]. Recently, bacterial virulence properties have been revisited as attractive targets for the development of new therapeutic agents[26,27]. In such a perspective, type IV pili represent particularly appealing virulence factor targets. They are associated with a remarkable array of properties ranging from motility to electric conductance, and are arguably one of the most widespread virulence factor since distinctive proteins dedicated to their biogenesis are found in most known species of prokaryotes[2].

This study demonstrates that trifluoperazine and thioridazine rapidly impair functions carried by type IV pilus structures, including twitching motility, aggregation, or adherence to inert or cell surfaces in model bacterial pathogens: *Neisseriae* species and *Pseudomonas aeruginosa*. In an *in vivo* model of meningococcal infection, when administered after infection at doses compatible with use in humans, thioridazine reduces bacterial colonisation of blood vessels, as well as vascular alterations, thrombosis and inflammation, the hallmarks of invasive meningococcal infections. Furthermore, in agreement with our recent observation that colonization of blood vessels by piliated meningococci is required for sustained bacteremia responsible for sepsis and subsequent lethality[19], thioridazine reduces bacteremia and increases mice survival. In association with antibiotics, it reduces vascular inflammatory and thrombotic responses that were shown to be highly detrimental and correlated with the severity of the disease in patients[16,17,28]. Altogether, our results demonstrate *in vivo* the efficacy of these compounds in reducing the pathogenic consequences of a bacterial infection relying on type IV pilus expression.

Before extensive use as neuroleptics, phenothiazines were first reported as antimicrobial agents against Gram-positive and Gram-negative bacteria[29]. However, phenothiazines, and more particularly thioridazine, have only modest antimicrobial activity, at concentrations and time scale beyond those impacting type IV pilus functionality[30]. In consistence with previous observation that phenothiazines potently inhibit efflux pumps in both human and microorganisms[31], our data strongly suggest that phenothiazines target Na^+-NQR. This protein complex, highly conserved among numerous non-pathogenic and pathogenic bacteria, catalyzes the oxidation of NADH and the reduction of quinone. The released energy drives a sodium motive force through the translocation of Na+ across the inner cell membrane. In many pathogenic bacteria, Na+ gradient is an entry site for electrons into the respiratory chain towards ATP synthesis, or to sustain ionic homeostasis, nutrient transports, flagellum rotation and other essential processes[21,32]. In *Vibrio cholerae,* Na^+-NQR was

shown as physiologically ubiquitous, including motility and formation of bacterial monolayers, an initial step in the build-up of biofilms[33,34]. The recent approach used to identify genes essential for meningococcal pathogenesis unraveled a role of the *nqr* complex for colonization of the human blood vessels[19]. However, no link with type IV pili functionality had been reported so far. How this sodium gradient affects type IV pilus dynamics remains to be explored. The mechanisms promoting the ATPase-driven elongation/retraction cycles remains elusive. Model system suggests that pilus retraction proceeds as pilin subunit monomers are disassembled from the base of an extended type IV pilus polymer and dispersed into the membrane for later reuse in pilus elongation[3,20]. Retraction can occur in two distinct speed modes, an unusual motor property conserved between different bacterial species[35,36], and switching between retraction and elongation occurs at different time scales[35]. In *N. gonorrhoeae*, oxygen depletion triggers speed switching from the high to the low speed mode, resulting in the disassembly of gonococcal microcolonies within minutes[37]; such effect is most likely occurring by controlling proton motive force and, in the end, changes in the pilus-pilus interaction force[38]. As the sodium gradient generated by the Na^+-NQR can provide an entry site for electron into the respiratory chain for ATP synthesis[21,32], phenothiazines might affect proton motive force resulting in the switch of pilus retraction mode. Furthermore, one might not exclude the possibility that periplasmic Na^+ fine-tunes the activity of proteins promoting pilus stability[7]. Further studies will be required to fully characterize the mode of action of sodium gradient on pilus dynamics.

In our mice model, trifluoperazine was effective *in vivo* on bacterial clearance and vascular lesions at doses 10 fold higher than recommended for chronic administration in humans, and we observed some toxicity in septic animals even in the presence of cefotaxime. However, thioridazine was very well tolerated and effective at dose regimen compatible with human use. It is therapeutically safe with few side effects when used with moderation, as proven by the 60 plus years it has been in use[39]. We showed that it reduced vascular lesions and improved mice survival in the absence of antibiotic treatment when administrated early during the infection. These tests should also be extended to other related phenothiazines, such as mezoridazine or promazine, which were also very effective *in vitro*. Although it is difficult to predict from mice study how effective thioridazine and other related compounds might be on the outcome of an infection in human, we believe that it could prevent some of the deleterious consequences of the infections by bacterial pathogens relying on type IV pili expression. The role of Tfp in adhesion to host cells, aggregation, biofilm formation is crucial for pathogenesis of numerous human pathogens, such as enteropathogenic *Escherichia coli* EPEC[40], *P. aeruginosa resistance*[41] *or* nontypeable *Haemophilus influenza*[42]. Interfering with type IV pilus-mediated host cell interaction therefore represents an

368 attractive strategy to modify the course of diseases induced by these pathogens. Due to the well-
369 conserved set of proteins involved in type IV pilus biosynthesis in Gram-negative bacteria, it is most
370 likely that phenothiazines may also act on numerous other type-IV piliated pathogenic bacteria.
371
372 Taken together, through an unexpected regulation of bacterial type IV pili expression by
373 phenothiazines, this work reveals a new approach to reduce meningococcal vascular colonization and
374 subsequent vascular lesions and lethality, as well as the benefit of such molecules as adjuvant
375 therapy for the treatment of invasive meningococcal disease. This provides proof of concept that
376 compounds with an activity against bacterial type IV pili could be used in addition to antibiotics to
377 prevent and treat bacterial diseases.
378

METHODS

Antibodies and Reagents

The list of the antibodies used in this work is provided in supplementary Table 3. mAb raised against PilE (20D9) and polyclonal antiserum raised against meningococcal 2C4.3 strain were described previously[9]. DAPI, Trifluoperazine (T8516), Fluphenazine (F4765), Prochlorperazine (P9178), Perphenazine (P6402), Thioridazine (T9025), Mesoridazine (M4068), Chlorpromazine (C8138), Promazine (P6656), Triflupromazine (1686003) and Levomepromazine (L0500000) were purchased from Sigma Aldrich. Phalloidin coupled to Rhodamin or Alexa Fluor 633 were purchased from Interchim and Invitrogen, respectively. Gentamicin was purchased form Gibco and Cefotaxime from Mylan.

Bacterial strains

Nm 2C4.3 (formerly clone 12) is a piliated capsulated Opa$^-$ Opc$^-$ variant of the serogroup C meningococcal clinical isolate 8013[43]. The isogenic derivative mutants ΔPilT, where the *pilT* gene was interrupted by an erythromycin-resistance cassette and the isogenic strain harbouring an IPTG-inducible *pilC1* gene (*pilC1*$_{ind}$) were previously described[20,44]. Transposon insertions in individual nqr genes were recovered from the genome-wide collection of *N. meningitidis* transposition mutants[45] and isogenic 2C4.3 mutants were generated by transformation. Z5463 (formerly C396) is a capsulated, piliated OpaA$^+$ Opc$^+$ meningococcal clinical isolate of serogroup A[46]. FAM20 is a capsulated, piliated, Opa$^-$, Opc$^-$ strains of serogroup C[47]. Meningococci were cultured as described previously[48]. Briefly, before experiments, bacteria were grown overnight on GCB solid medium (4% GC medium base; Difco), 1% agar, 0.4% glucose, 0.2 mg/ml thiamine, 0.0005% Fe(NO3)39H2O, 0.01% L-glutamine at 37°C under 5% CO2. Several colonies were then selected and grown in DME supplemented with 0.1% BSA for 2h and were finally diluted to 10^7 bacteria/ml suspension for cell infection.

Three different strains of *Neisseria gonorrhoeae* were used: the reference strain MS11 and two other strains FAT1.1 and SB2ST11. Bacteria were grown for approximately 36h on chocolate agar plates. Several colonies were then selected and grown for 2h in DMEM supplemented with 0.1% BSA and adjusted to an optical density (OD) of 0.1 before experiment. The strain *Pseudomonas aeruginosa* PAO1 and its derivative expressing the fluorescent protein mCherry were kindly provided by Dr Mylène Robert-Genthon (CEA Grenoble, France). PAO1 strains were grown in LB medium (supplemented with Tetracycline to maintain m-Cherry expression) overnight at 37°C on a shaker before experiments.

Bacterial growth assays

Growth of *Nm* 2C.43 in the presence of trifluoperazine or thioridazine was measured at 600 nm at intervals of 1h up to 6h with a spectrophotometer. To measure bactericidal activity, a bacterial suspension of *Nm* 2C4.3 at optical density (OD) 0.1 was distributed in 24-well plate (1ml/well). After 1 hour of incubation, trifluoperazine, thioridazine, gentamicin, cefotaxime or PBS alone as control were added. After 15 min treatment, serial dilutions were performed in physiological water and 100 µl of each dilution were plated on GCB solid media (BD, Difco GC media) containing supplements, incubated overnight and the colonies were counted.

Bacterial aggregation assays

Bacteria were grown in liquid culture for 2h to form bacterial aggregates before the indicated treatment, i.e. increasing concentrations of trifluoperazine (10 to 40 µM), thioridazine (1 to 10 µM), gentamicin (150 µg/ml) or cefotaxime (20 µg/ml) for 30 minutes. When indicated, bacteria were grown in liquid culture for 2h to form bacterial aggregates, then NaCl was added to reach concentrations varying from 6,4 g/L to 21,4 g/L, before treatment with trifluoperazine or thioridazine. Bacterial aggregates were visualized using a phase-contrast microscope. Quantification analysis of the size of bacterial aggregates was performed using ImageJ software.

To assess *P. aeruginosa* twitching and swarming motility, *P. aeruginosa* PAO1 strain was grown for 24h in low-agar (0.5%) medium enabling bacterial swarming (dependent on flagellum) and in high-agar (1%) medium, enabling type IV pilus dependent twitching motility, as previously described[49]. *P. aeruginosa* PAO1 strain expressing mCherry was grown for 3 days on a solid surface under flow (2 dynes/cm^2) to promote biofilm maturation and growth of the three-dimensional community and trifluoperazine (100 µM) was applied for 2 h under flow. Bacteria were fixed and the fluorescent biofilm was analysed by confocal microscopy at 20x and 100x. Surface of the fluorescent biofilm (in pixel ²) was measured using ImageJ software.

Generation and whole genome sequencing analysis of bacterial resistant strains

To generate strains resistant to the action of phenothiazines, one clone of *N. meningitidis* 2C.43 was selected by performing 3 passages on GCB solid medium, bacteria were grown in the presence of 40 µM trifluoperazine over 3 passages, then 10^8 were plated GCB solid medium containing 50 µM trifluoperazine. Out of the 13 recovered resistant clones, 4 clones were still forming aggregates in suspension, and these aggregates were now resistant to the dispersal effect of both trifluoperazine (40 µM) and thioridazine (4 µM). Genomic DNA was extracted using DNeasy Blood and Tissue Kit. Genomic libraries were prepared using a Nextera XT kit, multiplexed and sequenced on an Illumina MiniSeq instrument (2x150 paired-end sequencing). Single nucleotide polymorphisms (SNPs) and small indels were assessed using Snippy v3.1 (https://github.com/tseemann/snippy). Briefly, Snippy

was used to map the raw short reads of C2, C4, C8 and C13 clones against the annotated assembly of the parental strain (*Neisseria meningitidis* 8013 NC_017501.1). SNP variants were confirmed by PCR amplification and Sanger sequencing of the corresponding genes. The sequences reported in this paper are available at NCBI's BioProject database under accession number PRJNA481885 (http://www.ncbi.nlm.nih.gov/bioproject/481885).

Cell culture and infection

Primary Human Dermal Microvascular Endothelial Cells (HDMEC) isolated from the dermis of juvenile foreskin and adult skin (different locations) and their specific endothelial cell growth medium were purchased from PromoCell. hCMEC/D3, engineered in the team of Pierre-Olivier Couraud at the Institut Cochin, is a fully differentiated human brain endothelial cell line derived from brain capillaries, which recapitulates the major phenotypic features of the blood-brain barrier[50]. HCMEC/D3 cells were grown in EBM-2 basal medium (Lonza, Walkersville, MD, USA) supplemented with 5% Fetal Bovine Serum "Gold", 10 mM HEPES (PAA Laboratories GmbH, Pasching, Austria), 1% Penicillin-Streptomycin, 1% chemically defined lipid concentrate (Invitrogen Ltd**,** Paisley, UK), 1.4µM hydrocortisone, 5 $\mu g.ml^{-1}$ ascorbic acid and 1 $ng.ml^{-1}$ bFGF (Sigma-Aldrich, St. Louis, MO). They were tested for mycoplasma contamination. When indicated, HDMECs were split on channel slides (µ-slide I Luer from *ibidi*), grown for 2 days to reach confluency and then subjected to a laminar flow shear stress (10 dynes/cm^2) for 4 days (*ibidi* Pump System, *ibidi*). To infect cells, bacteria were precultured in prewarmed cell culture medium for 1h 30 min at 37°C under 5% CO_2 atmosphere. The OD_{600} was adjusted to 0.1 and cells were then overlaid with bacteria for 30 min (MOI of 100). Unbound bacteria were removed by three washes in cell culture media and infection was allowed to proceed for 1h at 37°C 5% CO_2 before treatment with trifluoperazine or thioridazine for 20 min. Cells were then washed and fixed in 4% paraformaldehyde for immunofluorescence analysis.

Immunofluorescence microscopy and live imaging

HDMEC or hCMEC/D3 cells were grown to confluence on Thermanox coverslips (Thermo Fischer Scientific) or ibidi device. After the indicated treatments and/or infection, cells were washed, fixed in 4% paraformaldehyde and immunostaining was performed with the indicated primary and secondary antibodies. Image acquisitions were performed on a Leica DMI6000. Quantification were done using ImageJ software (NIH). For time lapse video microscopy, bacteria grown for 2h in liquid culture medium or on cells, and image acquisitions before and after addition of trifluoperazine were performed overtime, at one frame per second for 20 minutes, on a Leica DMI6000 with Yokogawa CSU-X1M1 system and CoolSnap HQ2 (Photometrics). Image sequences were processed with ImageJ software to create the videos.

Matrix degradation assay

Thermanox coverslips (Thermo Fischer Scientific) were washed in ethanol 70%, dried then coated with poly-L-lysine 1 mg/ml for 20 min at room temperature. After one wash in sterile PBS, 0.5% glutaraldehyde was added for 15 min at room temperature. After three washes in PBS, gelatin-FITC (G13187 from Invitrogen) was added at 0.2 mg/ml for 10 minutes at room temperature in the dark. Coverslip were then washed with sterile PBS and treated with 5 mg/ml sodium borohydride for 3min. After three washes in sterile PBS, 10^5 HDMECs were seeded per well in their PromoCell culture medium and incubated overnight at 37°C 5% CO_2. The day after, cells were infected with *Neisseria meningitidis* 2C4.3, as described above. Infection was allowed to proceed for 6h before gentamicin treatment at 150 mg/ml for 1h. After three washes in cell culture medium, trifluoperazine or thioridazine was added for 20 min, washed with the culture medium and were incubated overnight in cell culture media containing 15 mg/ml Gentamicin. Cells were then fixed in 4% Paraformaldehyde for 10 min, stained with phalloidin and DAPI for 1 hour and mounted in glycergel (DAKO). Image acquisitions were performed on a Leica DMI6000 with Yokogawa CSU-X1M1 system and CoolSnap HQ2 (Photometrics). Quantifications were performed using ImageJ software (NIH).

Scanning Electron Microscopy analysis (SEM)

HDMECs grown on glass coverslips were infected with meningococci for 1 h and treated with trifluoperazine or thioridazine, as described above, fixed with 4% paraformaldehyde for 10 min, treated with 1% osmium tetroxide in water, in the dark for 1 h and dehydrated with increasing ethanol concentration baths before drying with a critical point drier (Quorum Technologies K850, Elexience, France). Dry coverslips were mounted on stubs, coated with 5 nm platinum (Quorum Technologies Q150T, Elexience, France) and observed with a Zeiss SEM Merlin Compact VP (Zeiss, France).

Transmission electron microscopy

Bacteria were grown in liquid culture medium for 2h, Trifluoperazine (or control vehicle) was added at 40 µM for 20 min, bacterial suspensions were then fixed in 4% paraformaldehyde for 10 min, centrifuged at 1000 rpm for 5 minutes and the bacterial pellets washed in PBS. After negative staining with 1% phosphotungstic acid, bacteria were analysed by transmission electron microscopy, using a JEOL 1011 microscope.

Stochastic Optical Reconstruction Microscopy (STORM)

Bacteria were grown in liquid culture medium for 2h, Trifluoperazine (or control vehicle) was added at 40 µM for 30 min, then bacterial suspensions were fixed in 4% paraformaldehyde/0.2% glutaraldehyde for 10 min, centrifuged at 850 g for 5 min and the bacterial pellets washed in PBS, permeabilized with PBS/0.05% saponin, washed, blocked with PBS/BSA 2% for 10 min, labeled with the anti-PilE antibody in PBS/BSA 2%/saponin 0.05%- for 1h, washed, then incubated with goat anti-mouse Alexa Fluor 647 F(ab')2 secondary antibody fragments (Life Technologies, A-21237) (1:500) for 1h. Labeled preparations were centrifuged on microscope slides using a cytospin, post-fixed in PBS/formaldehyde 3,6% for 15 min, washed in PBS then mounted on slide with cavities (Marienfield) in Abbelight dSTORM super resolution buffer and sealed with a twinsil 22 silicon-glue (Rotec) as previously described[11]. Imaging was performed on a Leica SR GSD 3D system, with a 160x oil (NA 1.43) objective. Fluorescence was collected onto an EMCCD camera iXon Andor technology, providing an effective pixel size of 100 nm and processed with the LAS X software (Leica). Approximately 50,000 frames were recorded for each acquisition with 20 ms exposure time, EM gain of 250 and the number of photons per pixels set to 50. 2D reconstructions were obtained from stacks (16 planes) with 50 nm axial step size, using LAS X software (Leica).

Infection of human brain tissues

The effect of trifluoperazine on the colonization of human brain vessels, using an *ex vivo* meningococcal infection model of fresh human frontal brain tissues was performed as described previously[10]. In this setting, histological and anatomical characteristics of the brain vessels were conserved. Meningococci incubated with tissue sections established specific tight association with brain vessels, reminiscent of neuropathological findings in patients with meningococcal meningitis and adhesion relying on the expression of type IV pili[10]. Fresh human brain sections, provided by Prof. Fabrice Chretien (Poincaré Hospital and Institut Pasteur, Paris), were obtained from frontal lobe specimens of macroscopically and histologically normal brain (confirmed by a neuropathologist) of individuals referred to the Department of Forensic Medicine for unexplained out-of-hospital sudden death (consent forms ML1094, PFS 10-008, ClinicalTrials.gov NCT00320099 from The Institutional Review Boards of the Poincaré Hospital, Versailles-Saint Quentin University and the French "Agence de la Biomédecine"). After freezing of the brain tissue with isopentane cooled in liquid nitrogen, the sections (7 µm thick) containing leptomeninges, cortical ribbon and the underlying white matter were immobilised on superfrost™ plus microscope slides and stored at -80°C. Defrosted sections were rehydrated in PBS for 5 min and incubated for 1h with medium containing 0.1% BSA prior to infection with suspensions of bacteria ($2x10^7$ bacteria in 150µl of medium containing 0.1% BSA) for 1h at 37°C. Sections were then treated for 30 min with Trifluoperazine 30 µM or PBS alone as a

control and were then gently washed horizontally 5 times and fixed in PAF 4% for 10 min at RT. Adherent meningococci were detected by immunofluorescence analysis. Brain sections were incubated with the anti-human CD31/PECAM-1 mouse monoclonal antibody and a rabbit polyclonal serum anti-*Nm* 2C4.3 strain for 2h in PBS/BSA 0.1%. Alexa-conjugated Phalloidin and DAPI were added to Alexa-conjugated secondary antibodies for 1h. After additional washing, coverslips were mounted in glycergel (Dako). Entire samples were scanned using a Lamina multilabel slide scanner (PerkinElmer) and were further analysed using confocal microscopy (spinning disk Leica, 63x). Quantification analysis of the images (n=50 per section) was performed using ImageJ software (NIH). Results are presented as a vascular colonisation index corresponding to the area occupied by the fluorescently labelled bacteria in relation to the human vessel area delineated by the anti-PECAM-1/CD31 staining, from 2 independent sections per condition.

Infection of SCID mice grafted with human skin

Six week old CB17/Icr-*Prkdc*^{scid} (Severe Combined Immunodeficiency: SCID) female mice were obtained from Janvier Labs (Saint-Berthevin, France). Human skin tissues were obtained from adult patients undergoing plastic surgery in the Service de Chirurgie Plastique et Reconstructive of the Groupe Hospitalier Saint-Joseph (Paris, France). In accordance with the French legislation, patients were informed and did not refuse to participate in the study. Experimental procedures were performed as previously described[18], in accordance with the guidelines of the Institut National de la Santé et de la Recherche Médicale and were conformed to the European ethical legislation (Directive 2010/63/EU). The experimental protocol was approved by the Animal Experimentation Ethics Committee of the Université Paris Descartes (consent forms CEEA34.O.J.L.039.12 and 2018012515596498). Briefly, mice were prepared for transplantation by shaving the hair of the back and abdominal areas after an intraperitoneal injection of ketamine 100 mg.kg^{-1} and xylazine 10 mg.kg^{-1}. A skin flap was created and a full thickness human skin graft was placed onto the wound bed. The transplants were held in place with 6-0 nonabsorbable monofilament suture materials, and the flap was then sutured above the transplant. Four to six weeks after human skin transplantation, grafted mice were randomized into control and treated groups for meningococcal infection experiments. *N. meningitidis* strains were grown overnight at 37 °C on GCB agar plates prepared without iron and supplemented with 15 µM deferoxamine (Desferal, Novartis) with appropriate antibiotic when required. Bacterial colonies were harvested and cultured in RPMI with 1% bovine serum albumin medium and 0.06 µM deferoxamine with gentle agitation to reach the exponential phase of growth. Bacteria were then resuspended in physiological saline solution. Mice were infected intravenously with 100 µl ($5x10^6$ bacteria) of this bacterial suspension. Ten mg of human holotransferrin (R&D Systems) was administered intraperitoneally just before infection. 2h after

bacterial challenge, trifluoperazine (40 mg/kg), thioridazine (4 mg/kg) or vehicle as a control were administrated intraperitoneally and mice were sacrificed at 4h after infection. When used alone or in combination with cefotaxime, thioridazine was administrated subcutaneously and cefotaxime (200 mg/kg) was administrated intraperitoneally to avoid precipitation. Cefotaxime was re-administrated subcutaneously at 18h and 42h after bacterial challenge. To assess bacteremia in infected animals, 10 µl of blood was sampled using a heparinized hematocrit glass tube 1h after injection by puncture in the lateral tail vein, or 4h after injection by intracardiac puncture on animal sacrificed by intraperitoneal injection of a lethal dose of ketamine and xylazine. 10 µl of blood was used for bacterial counts performed by plating serial dilutions of blood on GCB agar plates. Results were expressed in colony-forming units (CFU) per ml of blood. The remaining blood was centrifuged (3000 rpm for 20 min at 4°C) and sera were collected and frozen at -80 °C. Human skin grafts were carefully collected in RNA later (Sigma-Aldrich), half of the graft was cut into small pieces using sterile cutter, before lysis in TRI-Reagent for RNA preparation. The rest of the tissue was washed in PBS and fixed overnight at 4 °C in 4% paraformaldehyde in phosphate buffer. After washing in phosphate buffer, the specimens were embedded in OCT and then frozen at -80°C. 7 µm thick sections of the dermis were immobilised on superfrost^{TM} plus microscope slides and proceeded for hematoxylin and eosin staining or immunofluorescence analysis. Sections were incubated with the primary antibodies for 1h in PBS/BSA 3% then DAPI was added to Alexa-conjugated secondary antibodies for 1h. After additional washing, coverslips were mounted in glycergel (Dako), entire samples were scanned using a Lamina multilabel slide scanner (PerkinElmer) and were further analysed using confocal microscopy (spinning disk Leica, 63x). Quantification analysis of the images was performed using ImageJ software (NIH). Results are presented as a vascular colonisation or thrombosis index corresponding to the area occupied by the fluorescently labelled bacteria or platelets in relation to the human vessel area delineated by the anti-collagen IV (n= 30 to 50 vessels per graft from 3 to 7 independent grafts per condition).

Quantitative Real-Time PCR analysis

Tissues or cells were kept at -80°C with TRI-Reagent (Sigma Aldrich). RNA were extracted with the TRI-Reagent phenol/chloroform method; cDNAs were synthesized using Superscript II reverse-transcriptase kit (Life Technologies). RT-qPCR were performed using SyberGreen system (Roche Diagnostics) and the endothelial cell marker gene PECAM-1/CD31 was used to normalize the expression of the other genes. Relative changes in mRNA expression were calculated using the comparative cycle method ($2^{-\Delta\Delta Ct}$). The list of primers used in this work is provided in supplementary Table 4.

Multiplex electrochemiluminescent immunoassays

The serum concentrations of human inflammatory cytokines were quantified by electrochemiluminescence using multiplex assay kits from Meso Scale Discovery. 25 µl of serum were added to the 96-well MULTI-SPOT plates and the assays were processed following the manufacturer's instructions. Plates were read on the multiplexing imager Sector S600 (Meso Scale Discovery).

The serum concentrations of cytokines produced might vary between experiments, depending on the skin grafts (different donors, the number of connected vessels contained within the graft) and/or the levels of bacteremia. However, the inhibitory effects of phenothiazines was quite similar among experiments, with a reduced inflammation varying from 50 to 70%.

Statistical analysis

Statistical significance was assessed with the Student's *t*-test and one way-ANOVA by Prism software.

Data availability

Data supporting the findings of this study are available within the paper and its supplementary information files. The sequences of the SNP variants resistant to the action of phenothiazines are available at NCBI's BioProject database under accession number PRJNA481885 (http://www.ncbi.nlm.nih.gov/bioproject/481885).

Acknowledgments

We thank Mylène Robert-Genthon and Fabrice Chretien for providing *P. aeruginosa PAO1* strain and brain tissues; Maryline Favier of the histology facility, Alain Schmitt and Thomas Guilbert of the imaging facility, Karine Bailly and Muriel Andrieu of the cytometry facility of the Institut Cochin for their expert technical help.

K.D. and L.LG. were supported by a doctoral fellowship from la Region Ile de France and the Fondation pour la Recherche Médicale, respectively. This work was supported by a collaborative research grants from the Agence Nationale de la Recherche of France (ANR-14-IFEC14-0006) to S.B. and X.N. in the framework of the Infect-ERA joint transnational call (European funding for infectious diseases research), by the Société d'Accélération du Transfert de Technologie (ANR-10-SATT-05-01) to S.B. and by grant ANR 10-EQPX-04-01 to F.L.

Additional information

The authors declare no competing financial interests.

REFERENCES

1. Pelicic, V. Type IV pili: e pluribus unum? *Mol Microbiol* **68**, 827-837 (2008).
2. Berry, J.L. & Pelicic, V. Exceptionally widespread nanomachines composed of type IV pilins: the prokaryotic Swiss Army knives. *FEMS Microbiol Rev* **39**, 134-154 (2015).
3. Craig, L. & Li, J. Type IV pili: paradoxes in form and function. *Curr Opin Struct Biol* **18**, 267-277 (2008).
4. Kolappan, S*., et al.* Structure of the Neisseria meningitidis Type IV pilus. *Nat Commun* **7**, 13015 (2016).
5. Helaine, S*., et al.* PilX, a pilus-associated protein essential for bacterial aggregation, is a key to pilus-facilitated attachment of Neisseria meningitidis to human cells. *Mol Microbiol* **55**, 65-77 (2005).
6. Mikaty, G*., et al.* Extracellular bacterial pathogen induces host cell surface reorganization to resist shear stress. *PLoS Pathog* **5**, e1000314 (2009).
7. Brown, D.R., Helaine, S., Carbonnelle, E. & Pelicic, V. Systematic functional analysis reveals that a set of seven genes is involved in fine-tuning of the multiple functions mediated by type IV pili in Neisseria meningitidis. *Infect Immun* **78**, 3053-3063 (2010).
8. Stephens, D.S., Greenwood, B. & Brandtzaeg, P. Epidemic meningitis, meningococcaemia, and Neisseria meningitidis. *Lancet* **369**, 2196-2210 (2007).
9. Coureuil, M*., et al.* Meningococcus Hijacks a beta2-adrenoceptor/beta-Arrestin pathway to cross brain microvasculature endothelium. *Cell* **143**, 1149-1160 (2010).
10. Bernard, S.C*., et al.* Pathogenic Neisseria meningitidis utilizes CD147 for vascular colonization. *Nat Med* **20**, 725-731 (2014).
11. Maissa, N*., et al.* Strength of Neisseria meningitidis binding to endothelial cells requires highly-ordered CD147/beta2-adrenoceptor clusters assembled by alpha-actinin-4. *Nat Commun* **8**, 15764 (2017).
12. Coureuil, M*., et al.* Meningococcal type IV pili recruit the polarity complex to cross the brain endothelium. *Science* **325**, 83-87 (2009).
13. Coureuil, M., Lecuyer, H., Bourdoulous, S. & Nassif, X. A journey into the brain: insight into how bacterial pathogens cross blood-brain barriers. *Nat Rev Microbiol* **15**, 149-159 (2017).
14. Sokolova, O*., et al.* Interaction of Neisseria meningitidis with human brain microvascular endothelial cells: role of MAP- and tyrosine kinases in invasion and inflammatory cytokine release. *Cell Microbiol* **6**, 1153-1166 (2004).
15. Melican, K., Michea Veloso, P., Martin, T., Bruneval, P. & Dumenil, G. Adhesion of Neisseria meningitidis to dermal vessels leads to local vascular damage and purpura in a humanized mouse model. *PLoS Pathog* **9**, e1003139 (2013).
16. Girardin, E., Grau, G.E., Dayer, J.M., Roux-Lombard, P. & Lambert, P.H. Tumor necrosis factor and interleukin-1 in the serum of children with severe infectious purpura. *N Engl J Med* **319**, 397-400 (1988).
17. Waage, A., Brandtzaeg, P., Halstensen, A., Kierulf, P. & Espevik, T. The complex pattern of cytokines in serum from patients with meningococcal septic shock. Association between interleukin 6, interleukin 1, and fatal outcome. *J Exp Med* **169**, 333-338 (1989).
18. Join-Lambert, O*., et al.* Meningococcal interaction to microvasculature triggers the tissular lesions of purpura fulminans. *J Infect Dis* (2013).
19. Capel, E*., et al.* Peripheral blood vessels are a niche for blood-borne meningococci. *Virulence* **8**, 1808-1819 (2017).
20. Morand, P.C*., et al.* Type IV pilus retraction in pathogenic Neisseria is regulated by the PilC proteins. *Embo J* **23**, 2009-2017 (2004).
21. Juarez, O. & Barquera, B. Insights into the mechanism of electron transfer and sodium translocation of the Na(+)-pumping NADH:quinone oxidoreductase. *Biochim Biophys Acta* **1817**, 1823-1832 (2012).

22. Jeworrek, C*., et al.* Effects of specific versus nonspecific ionic interactions on the structure and lateral organization of lipopolysaccharides. *Biophys J* **100**, 2169-2177 (2011).
23. Lloret, J*., et al.* Ionic Stress and Osmotic Pressure Induce Different Alterations in the Lipopolysaccharide of a Rhizobium meliloti Strain. *Appl Environ Microbiol* **61**, 3701-3704 (1995).
24. Seebach, J*., et al.* Regulation of endothelial barrier function during flow-induced conversion to an arterial phenotype. *Cardiovasc Res* **75**, 596-607 (2007).
25. Levy, S.B. & Marshall, B. Antibacterial resistance worldwide: causes, challenges and responses. *Nat Med* **10**, S122-129 (2004).
26. Marra, A. Targeting virulence for antibacterial chemotherapy: identifying and characterising virulence factors for lead discovery. *Drugs R D* **7**, 1-16 (2006).
27. Felise, H.B*., et al.* An inhibitor of gram-negative bacterial virulence protein secretion. *Cell Host Microbe* **4**, 325-336 (2008).
28. van Deuren, M*., et al.* Correlation between proinflammatory cytokines and antiinflammatory mediators and the severity of disease in meningococcal infections. *J Infect Dis* **172**, 433-439 (1995).
29. Amaral, L*., et al.* Phenothiazines, bacterial efflux pumps and targeting the macrophage for enhanced killing of intracellular XDRTB. *In Vivo* **24**, 409-424 (2010).
30. Mazumder, R., Ganguly, K., Dastidar, S.G. & Chakrabarty, A.N. Trifluoperazine: a broad spectrum bactericide especially active on staphylococci and vibrios. *Int J Antimicrob Agents* **18**, 403-406 (2001).
31. Amaral, L., Engi, H., Viveiros, M. & Molnar, J. Review. Comparison of multidrug resistant efflux pumps of cancer and bacterial cells with respect to the same inhibitory agents. *In Vivo* **21**, 237-244 (2007).
32. Reyes-Prieto, A., Barquera, B. & Juarez, O. Origin and evolution of the sodium -pumping NADH: ubiquinone oxidoreductase. *PLoS One* **9**, e96696 (2014).
33. Van Dellen, K.L., Houot, L. & Watnick, P.I. Genetic analysis of Vibrio cholerae monolayer formation reveals a key role for DeltaPsi in the transition to permanent attachment. *J Bacteriol* **190**, 8185-8196 (2008).
34. Minato, Y*., et al.* Roles of the sodium-translocating NADH:quinone oxidoreductase (Na+-NQR) on vibrio cholerae metabolism, motility and osmotic stress resistance. *PLoS One* **9**, e97083 (2014).
35. Maier, B., Koomey, M. & Sheetz, M.P. A force-dependent switch reverses type IV pilus retraction. *Proc Natl Acad Sci U S A* **101**, 10961-10966 (2004).
36. Clausen, M., Jakovljevic, V., Sogaard-Andersen, L. & Maier, B. High-force generation is a conserved property of type IV pilus systems. *J Bacteriol* **191**, 4633-4638 (2009).
37. Kurre, R. & Maier, B. Oxygen depletion triggers switching between discrete speed modes of gonococcal type IV pili. *Biophys J* **102**, 2556-2563 (2012).
38. Dewenter, L., Volkmann, T.E. & Maier, B. Oxygen governs gonococcal microcolony stability by enhancing the interaction force between type IV pili. *Integr Biol (Camb)* **7**, 1161-1170 (2015).
39. Amaral, L. & Viveiros, M. Thioridazine: A Non-Antibiotic Drug Highly Effective, in Combination with First Line Anti-Tuberculosis Drugs, against Any Form of Antibiotic Resistance of Mycobacterium tuberculosis Due to Its Multi-Mechanisms of Action. *Antibiotics (Basel)* **6**(2017).
40. Bieber, D*., et al.* Type IV pili, transient bacterial aggregates, and virulence of enteropathogenic Escherichia coli. *Science* **280**, 2114-2118. (1998).
41. Persat, A., Inclan, Y.F., Engel, J.N., Stone, H.A. & Gitai, Z. Type IV pili mechanochemically regulate virulence factors in Pseudomonas aeruginosa. *Proc Natl Acad Sci U S A* **112**, 7563-7568 (2015).
42. Novotny, L.A*., et al.* Antibodies against the majority subunit of type IV Pili disperse nontypeable Haemophilus influenzae biofilms in a LuxS-dependent manner and confer therapeutic resolution of experimental otitis media. *Mol Microbiol* **96**, 276-292 (2015).

43. Nassif, X*., et al.* Antigenic variation of pilin regulates adhesion of Neisseria meningitidis to human epithelial cells. *Mol Microbiol* **8**, 719-725 (1993).
44. Pujol, C., Eugene, E., Marceau, M. & Nassif, X. The meningococcal PilT protein is required for induction of intimate attachment to epithelial cells following pilus-mediated adhesion. *Proc Natl Acad Sci U S A* **96**, 4017-4022 (1999).
45. Geoffroy, M.C., Floquet, S., Metais, A., Nassif, X. & Pelicic, V. Large-scale analysis of the meningococcus genome by gene disruption: resistance to complement-mediated lysis. *Genome Res* **13**, 391-398 (2003).
46. Achtman, M*., et al.* Purification and characterization of eight class 5 outer membrane protein variants from a clone of Neisseria meningitidis serogroup A. *J Exp Med* **168**, 507-525 (1988).
47. Dyer, D.W., McKenna, W., Woods, J.P. & Sparling, P.F. Isolation by streptonigrin enrichment and characterization of a transferrin-specific iron uptake mutant of Neisseria meningitidis. *Microb Pathog* **3**, 351-363 (1987).
48. Hoffmann, I., Eugene, E., Nassif, X., Couraud, P.O. & Bourdoulous, S. Activation of ErbB2 receptor tyrosine kinase supports invasion of endothelial cells by Neisseria meningitidis. *J Cell Biol* **155**, 133-143 (2001).
49. Burrows, L.L. Pseudomonas aeruginosa twitching motility: type IV pili in action. *Annu Rev Microbiol* **66**, 493-520 (2012).
50. Weksler, B., Romero, I.A. & Couraud, P.O. The hCMEC/D3 cell line as a model of the human blood brain barrier. *Fluids Barriers CNS* **10**, 16 (2013).

779 **FIGURE LEGENDES**

780 **Figure 1. Trifluoperazine inhibits bacterial aggregation**

781 **(a,b)** *N. meningitidis* 2C4.3 was grown in liquid culture for 2h to form bacterial aggregates and was
782 then treated with increasing concentrations of trifluoperazine (10 to 40 µM), gentamicin (150 µg/ml)
783 or cefotaxime (20 µg/ml) for 30 minutes. Bacterial aggregates were visualized using a phase-contrast
784 microscope. Images are representatives of 4 independent experiments performed in triplicate (scale
785 bars = 200 µm) (**b**) Quantification analysis of the size of bacterial aggregates was performed using
786 ImageJ software. (Mean ± SEM, n=3 experiments, *P <0.05, **P <0.01, ns non-significant ^{ns1}P=0.24,
787 ^{ns2}P=0.30 ; ^{ns3}P=0.14, One-way ANOVA Dunnett multiple comparison test. **(c)** *Nm* 2C4.3 wild type
788 strain and its isogenic derivative mutant ΔPilT grown in liquid culture for 2h to form bacterial
789 aggregates were treated with 50 µM trifluoperazine. Time lapse phase-contrast video microscopy
790 was performed to visualize the effect of trifluoperazine on bacterial aggregates over time. Images
791 were taken at the indicated time points of the video (see supplementary video 1) (scale bars = 200
792 µm). This experiment was repeated a minimum of 10 times with similar results. **(d)** The effect of
793 trifluoperazine treatment (50 µM) on twitching motility and bacterial aggregation was analysed over
794 time on *Nm* 2C4.3 bacterial aggregates using time lapse phase-contrast video microscopy and
795 movement tracking analysis (Imaris software). ~3 min after addition of the drug, twitching was
796 progressively lost, followed by the dispersion of the bacterial aggregates (~6 min after addition of the
797 drug). This experiment was performed twice with similar results.

798 **Figure 2. Trifluoperazine and Thioridazine regulate the piliation status of meningococci**

799 (**a**) *Nm* 2C4.3 wild type and the isogenic ΔPilT mutant grown in liquid culture for 2h to form bacterial
800 aggregates were treated with trifluoperazine (40 µM), thioridazine (4 µM) or PBS (Control) for 20
801 minutes, then fixed and stained with an anti-PilE antibody to visualize type IV pili and DAPI to
802 visualize bacteria. Images are representatives of 4 independent experiments (scale bars = 20 µm). (**b**)
803 Following treatment with trifluoperazine 40 µM for 20 minutes, bacteria were fixed and stained for
804 pilin PilE and analysed by an optical super-resolution (~20 nm) microscopy technique based on single-
805 molecule localization (dSTORM) on a Leica SR GSD. 50,000 frames were recorded for each
806 acquisition, reconstructed using the Leica Application Suite (LAS X) core module and merged with the
807 bright-field images of the same fields. Images are representatives of 3 independent experiments
808 (Scale bars = 2 µm). (**c**) *Nm* 2C4.3 wild type and the isogenic *ΔNqrA-F* mutants were grown in liquid
809 culture for 2h to form bacterial aggregates, then fixed and stained with an anti-PilE antibody to
810 visualize type IV pili and DAPI to visualize bacteria. Images are representatives of 2 independent
811 experiments (scale bars = 20 µm). (**d**) *N. meningitidis* 2C4.3 was grown in liquid culture for 2h to form

bacterial aggregates. NaCl or KCl was added to reach final concentrations varying from 6,4 g/L to 21,4 g/L. Bacteria were then treated with trifluoperazine (40 µM) or thioridazine (4 µM) for 20 min. Bacterial aggregates were visualized using a phase-contrast microscope. Images are representatives of 4 independent experiments performed in duplicates (scale bars = 100 µm).

Figure 3: Trifluoperazine and Thioridazine release bacteria from compact microcolonies formed on human endothelial cells

(a-c) HDMECs were infected with *Nm* 2C4.3 wild type and the isogenic ΔPilT mutant for 1h30, treated with trifluoperazine (10-40 µM), thioridazine (1-8 µM), gentamicin (150 µg/ml) or cefotaxime (20 µg/ml) for 30 minutes. (**a**) Cells were fixed and stained for cellular actin (phalloidin, red) and bacteria (anti-2C4.3, green) and analysed by fluorescent microscopy. Images are representatives of 4 independent experiments performed in triplicate (scale bars = 200 µm) (**b-c)** Quantification of the bacterial colonization by the wild type (**b**) and the isogenic ΔPilT mutant (**c**) was performed on 30 fields using ImageJ software. (**b**) Mean ± SEM, n=3 to 4 independent experiments, *P <0.05; **P <0.01; ***P<0.001; ns non-significant ^{ns1}P=0.36, ^{ns2}P=0.99 ; ^{ns3}P=0.49, One-way ANOVA Dunnett multiple comparison test. (**d)** HDMEC were infected with *Nm* 2C4.3 for 1h30, treated with trifluoperazine (40 µM), thioridazine (4 µM) or PBS (Control) for 30 minutes, fixed, and analysed once by scanning electron microscopy (scale bars = 20 µm). (**e**) Serial brain sections from the same donor were infected with *Nm* 2C4.3 for 1h30 to promote *in situ* adhesion to human brain vessels. Brain section were then treated with trifluoperazine (30 µM) for 30 min, washed, fixed and stained for the endothelial cell junction marker VE-cadherin (green), bacteria (red) and nuclei (blue), and the whole section was scanned using a Lamina scanner (Perkin Helmer). (**f**) Bacterial colonisation within the brain sections assessed by immunofluorescence analysis was quantified using ImageJ software as the ratio between bacterial surface colonisation in relation to the lumen surface of the vessels. 50 vessels per brain section were analysed. Mean of n=2 brain sections from 2 different donors.

Figure 4: Trifluoperazine and Thioridazine reduces bacteria-induced endothelial cell injury and matrix degradation

(**a**) HDMECs, grown under laminar shear stress (5 dynes/cm^2) for 5 days, were infected with *Nm* 2C4.3 wild type strain for 2h, treated with trifluoperazine (40 µM, 30 min), cefotaxime (20 µg/ml, 2h) or a combination of both. Cells were then fixed and stained for bacteria (red) and VE-cadherin (green), and analysed by confocal microscopy. Images are representatives of 3 independent experiments (scale bars = 50 µm). (**b-d**) HDMECs grown on fluorescent matrix (gelatin-FITC), were infected for 5h treated with increasing concentration of trifluoperazine (0-50 µM), thioridazine (0-4 µM) and 150 µg/ml gentamycin to prevent bacterial overload and subsequent cell death, due to

culture medium consumption, and cells were fixed 16h post-infection. Cells were stained for actin and analysed by confocal microscopy. The appearance of dark areas correspond to zones of matrix degradation. Images are indicative of three independent experiments performed in triplicate. (**c-d**) Gelatin degradation was quantified on 30 different fields using ImageJ software. (**c**) Mean ± SEM, n=3 independent experiments, ***P<0.001; One-way ANOVA. (**d**) Mean of n=2 independent experiments.

Figure 5: Trifluoperazine and Thioridazine induces bacterial clearance from human blood vessels *in vivo* and reduces signs of thrombosis, vascular injury and inflammation.

(**a-f**) Mice grafted with human skins were infected intravenously with *Nm* 2C4.3 wild type strain ($5x10^6$ bacteria). 2h after bacterial challenge, mice received 40 mg/kg trifluoperazine, 4 mg/kg thioridazine intraperitoneally or vehicle as a control. Mice were sacrificed at 4h post-challenge. This experiment was performed twice with n=3 or 4 mice per group, using skin from two different donors (n= indicate the number of mice per group). (**a**) Schematic representation of the different protocols used *in vivo*. (**b**) Control bacteremia 2h post-infection. Mean ± SEM. (**c**) Shown are representative images of the histological and immunofluorescence analysis of the skin grafts isolated from mice either non-infected or infected and treated with 40 mg/kg trifluoperazine, 4 mg/kg thioridazine at 2h post-challenge, or vehicle as a control. Top panel: Hematoxylin and eosin (HE) staining of the skin grafts, presenting signs of platelet and red blood cell aggregation in infected vessels. Middle panel: immunofluorescence analysis of the skin grafts showing the human vessels (Collagen IV, red) bacteria (green), platelet aggregation (pink) and nuclei (DAPI, blue). Lower panels: vascular integrity was assessed by immunofluorescence using markers of the endothelial cell junctions (PECAM-1 or VE-Cadherin, green) and bacteria (red). (**d**) Bacterial colonisation within the skin grafts assessed by immunofluorescence analysis was quantified using ImageJ software as the ratio between bacterial surface colonisation in relation to the lumen surface of the vessels. 30 to 50 vessels per mouse were analysed. Mean ± SEM, ***P<0.001; Two-tailed Student's *t*-test. (**e**) Thrombus formation within the skin grafts was assessed by immunofluorescence analysis and quantified using ImageJ as the ratio between thrombus surfaces in relation to the lumen surface of the vessels. 30 to 50 vessels per mouse were analysed. Mean ± SEM, *P<0.05, **P<0.01; Two-tailed Student's *t*-test. (**f**) Production of human cytokines (TNFα, IL-6, IL-8) in the mice sera was quantified with multiplex electrochemiluminescent immunoassays. 1 point correspond to one mice. Mean ± SEM from 2 independent experiments, *P <0.05, **P <0.01, ***P <0.001, ns non-significant, ns non-significant ^{ns1}P=0.36, ^{ns2}P=0.38 ; ^{ns3}P=0.11, One-way ANOVA Tukey's multiple comparison test.

Figure 6: Thioridazine improves the outcome of meningococcal infection alone or in combination with antibiotics.

879 (**a-d**) Mice grafted with human skin were infected intravenously with *Nm* 2C4.3 wild type strain
880 ($5x10^6$ bacteria); 2h after bacterial challenge, mice received thioridazine (4 mg/kg, subcutaneously),
881 cefotaxime (200 mg/kg, intraperitoneally) alone or in combination with thioridazine or vehicle as a
882 control. 18h and 42h after bacterial challenge, cefotaxime (200 mg/kg) was re-administrated
883 subcutaneously. This experiment was performed twice with n=3 or 4 mice per group, using skin from
884 two different donors (n= indicate the number of mice per group). This experiment was repeated 3
885 times with similar results. (**a**) Schematic representation of the protocol used *in vivo*. (**b**) Bacteremia
886 4h, 18h, 48h and 72h post-infection. Mean ± SEM. (**c**) Survival curve, *P= 0,028; Two sided log-rank
887 Mantel-Cox survival analysis. (**d**) Representative images of the histological analysis of the skin grafts
888 at 72h post-infection or at time of death (t.o.d. 18h) for the infected control mice. (**e-g**) Grafted mice
889 were infected intravenously with *Nm* 2C4.3 wild type strain; 2h after bacterial challenge, mice were
890 treated with cefotaxime alone or in combination with thioridazine, or vehicle as a control, and were
891 sacrificed at 4h post-infection. (**e**) Representative images of the histological and immunofluorescence
892 analysis of the skin grafts. Top panel: Hematoxylin and eosin (HE) staining of the skin grafts,
893 presenting signs of platelet and red blood cell aggregation in infected vessels. Lower panel:
894 immunofluorescence analysis of the skin grafts showing the human vessels (collagen IV, red) bacteria
895 (green), platelet aggregation (pink) and nuclei (DAPI, blue). (**f**) Bacterial colonisation and thrombosis
896 within the skin grafts at 4h post-post infection were assessed by immunofluorescence analysis and
897 quantified as described in Figure 5. Mean ± SEM, 40 vessels per mouse were analysed, n= 4 mice per
898 group, 40 vessels per mice **P<0.01, ***P<0.001, ^{ns}P=0.12; Two-tailed Student's *t*-test. (**g**)
899 Production of human cytokines in the mice sera was quantified with multiplex
900 electrochemiluminescent immunoassays. 1 point corresponding to one mice. Mean ± SEM from 2
901 independent experiments. ***P<0.001, ^{ns1}P=0.79, ^{ns2}P=0.09, ^{ns3}P=0.07, ^{ns4}P=0.16; Two-tailed
902 Student's *t*-test.

903

904

905

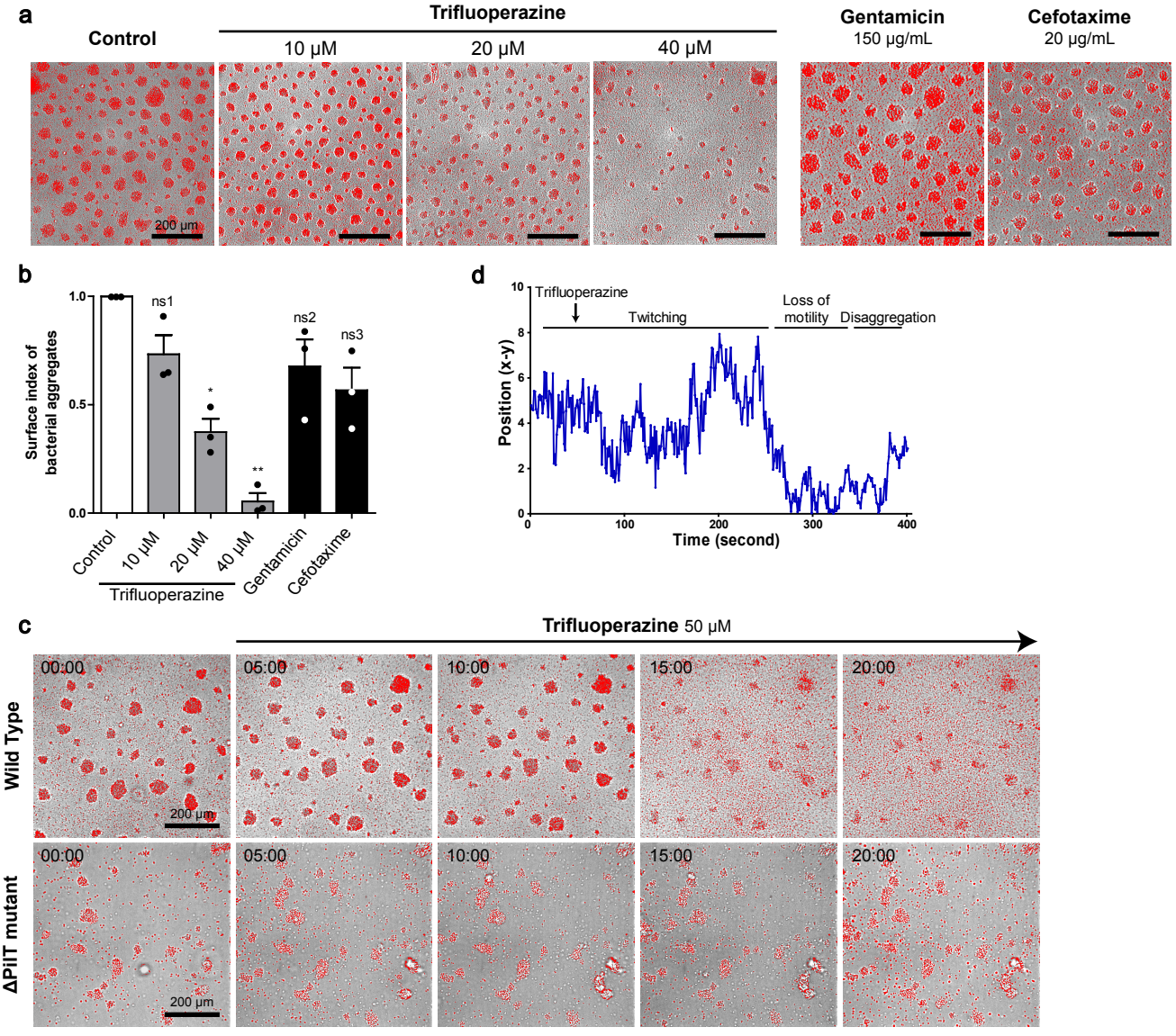
a
Control
Trifluoperazine
10 µM
20 µM
40 µM
Gentamicin
150 µg/mL
Cefotaxime
20 µg/mL
200 µm
b
Surface index of bacterial aggregates
1.0
0.5
0.0
ns1
*
**
ns2
ns3
Control
10 µM
20 µM
40 µM
Gentamicin
Cefotaxime
Trifluoperazine
d
Trifluoperazine
Twitching
Loss of motility
Disaggregation
Position (x-y)
Time (second)
c
Trifluoperazine 50 µM
Wild Type
ΔPilT mutant
00:00
05:00
10:00
15:00
20:00
200 µm

Figure 1

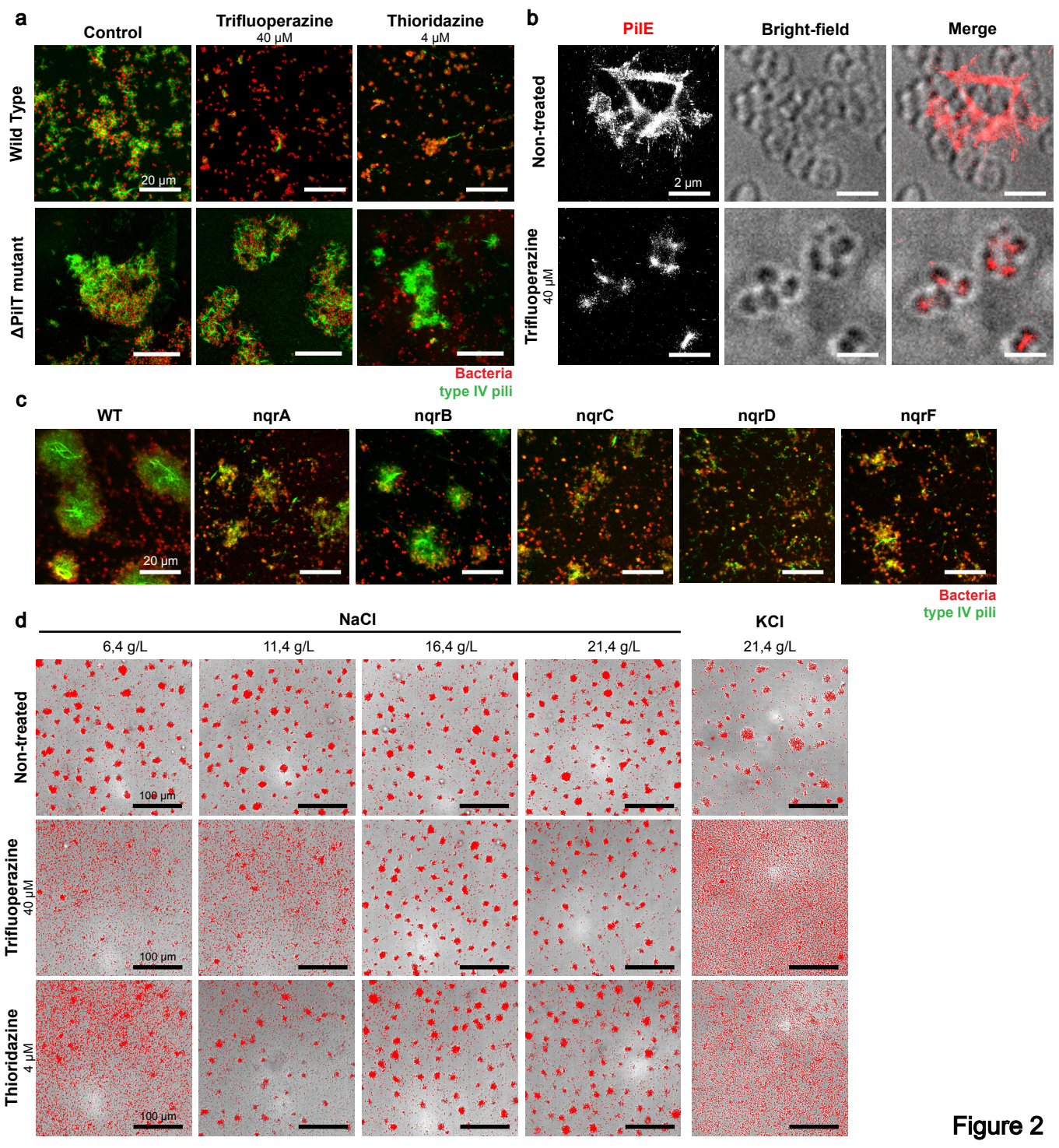
a
Control
Trifluoperazine
40 µM
Thioridazine
4 µM
Wild Type
ΔPilT mutant
20 µm
Bacteria
type IV pili
b
PilE
Bright-field
Merge
Non-treated
Trifluoperazine
40 µM
2 µm
c
WT
nqrA
nqrB
nqrC
nqrD
nqrF
20 µm
Bacteria
type IV pili
d
NaCl
KCl
6,4 g/L
11,4 g/L
16,4 g/L
21,4 g/L
21,4 g/L
Non-treated
Trifluoperazine
40 µM
Thioridazine
4 µM
100 µm

Figure 2

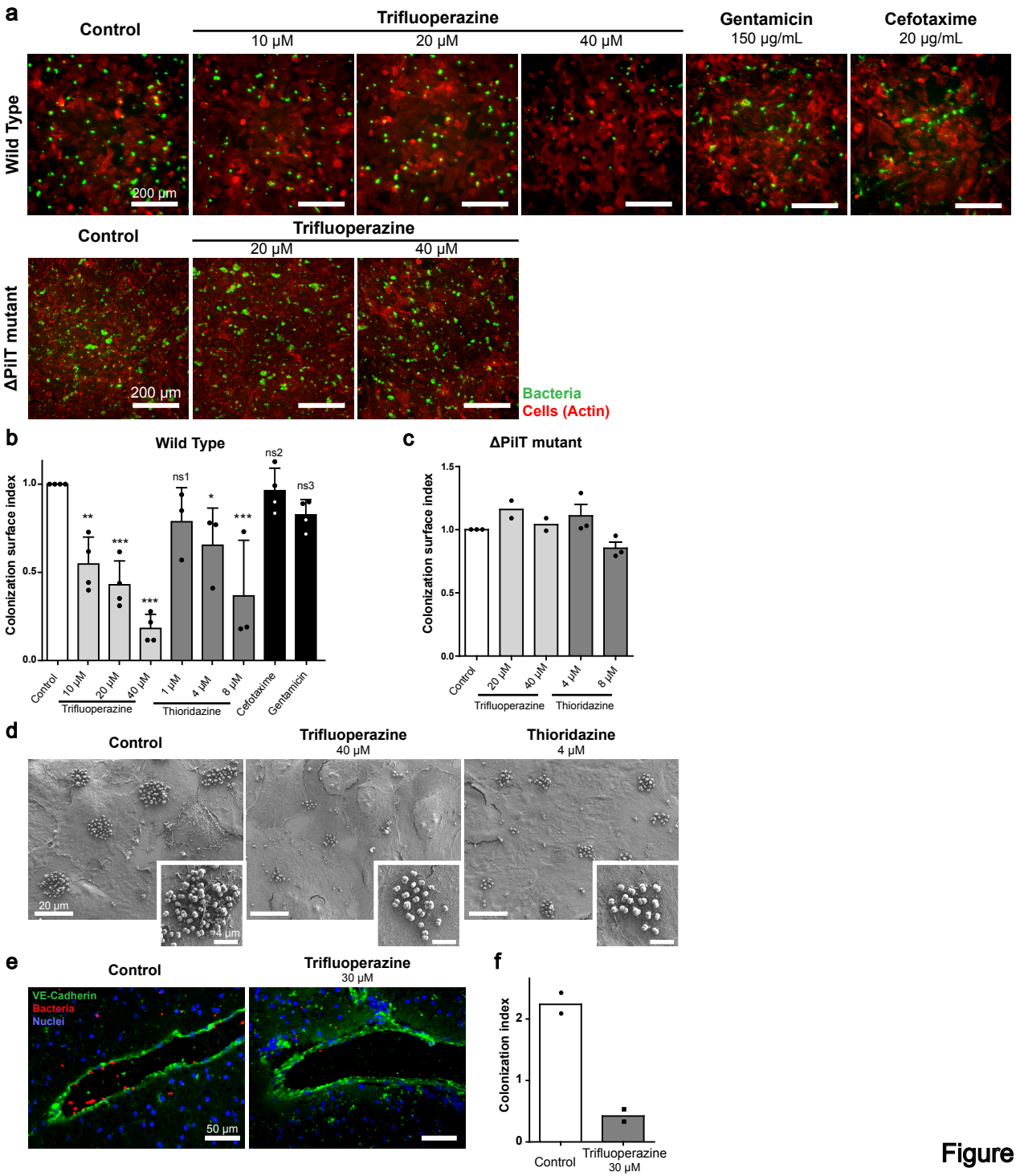
a
Control
Trifluoperazine
10 µM
20 µM
40 µM
Gentamicin
150 µg/mL
Cefotaxime
20 µg/mL
Wild Type
200 µm
Control
Trifluoperazine
20 µM
40 µM
ΔPilT mutant
200 µm
Bacteria
Cells (Actin)
b
Wild Type
Colonization surface index
1.0
0.5
0.0
**
***
***
ns1
*
***
ns2
ns3
Control
10 µM
20 µM
40 µM
1 µM
4 µM
8 µM
Cefotaxime
Gentamicin
Trifluoperazine
Thioridazine
c
ΔPilT mutant
Colonization surface index
1.5
1.0
0.5
0.0
Control
20 µM
40 µM
4 µM
8 µM
Trifluoperazine
Thioridazine
d
Control
Trifluoperazine
40 µM
Thioridazine
4 µM
20 µm
4 µm
e
Control
Trifluoperazine
30 µM
VE-Cadherin
Bacteria
Nuclei
50 µm
f
Colonization index
2
1
0
Control
Trifluoperazine
30 µM

Figure 3

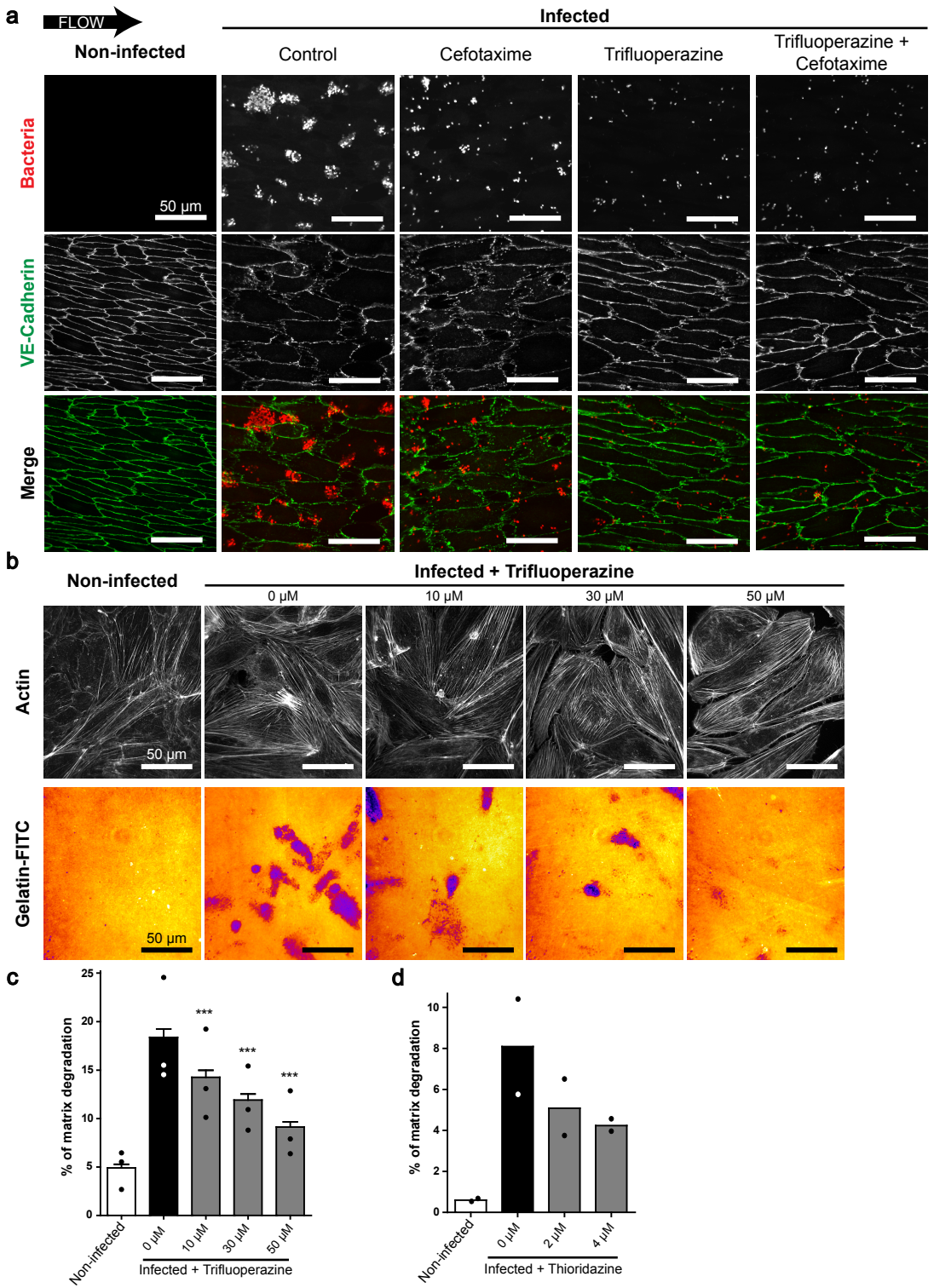
a
FLOW
Non-infected
Infected
Control
Cefotaxime
Trifluoperazine
Trifluoperazine + Cefotaxime
Bacteria
VE-Cadherin
Merge
50 µm
b
Non-infected
Infected + Trifluoperazine
0 µM
10 µM
30 µM
50 µM
Actin
Gelatin-FITC
50 µm
c
% of matrix degradation
***
Non-infected
0 µM
10 µM
30 µM
50 µM
Infected + Trifluoperazine
d
% of matrix degradation
Non-infected
0 µM
2 µM
4 µM
Infected + Thioridazine

Figure 4

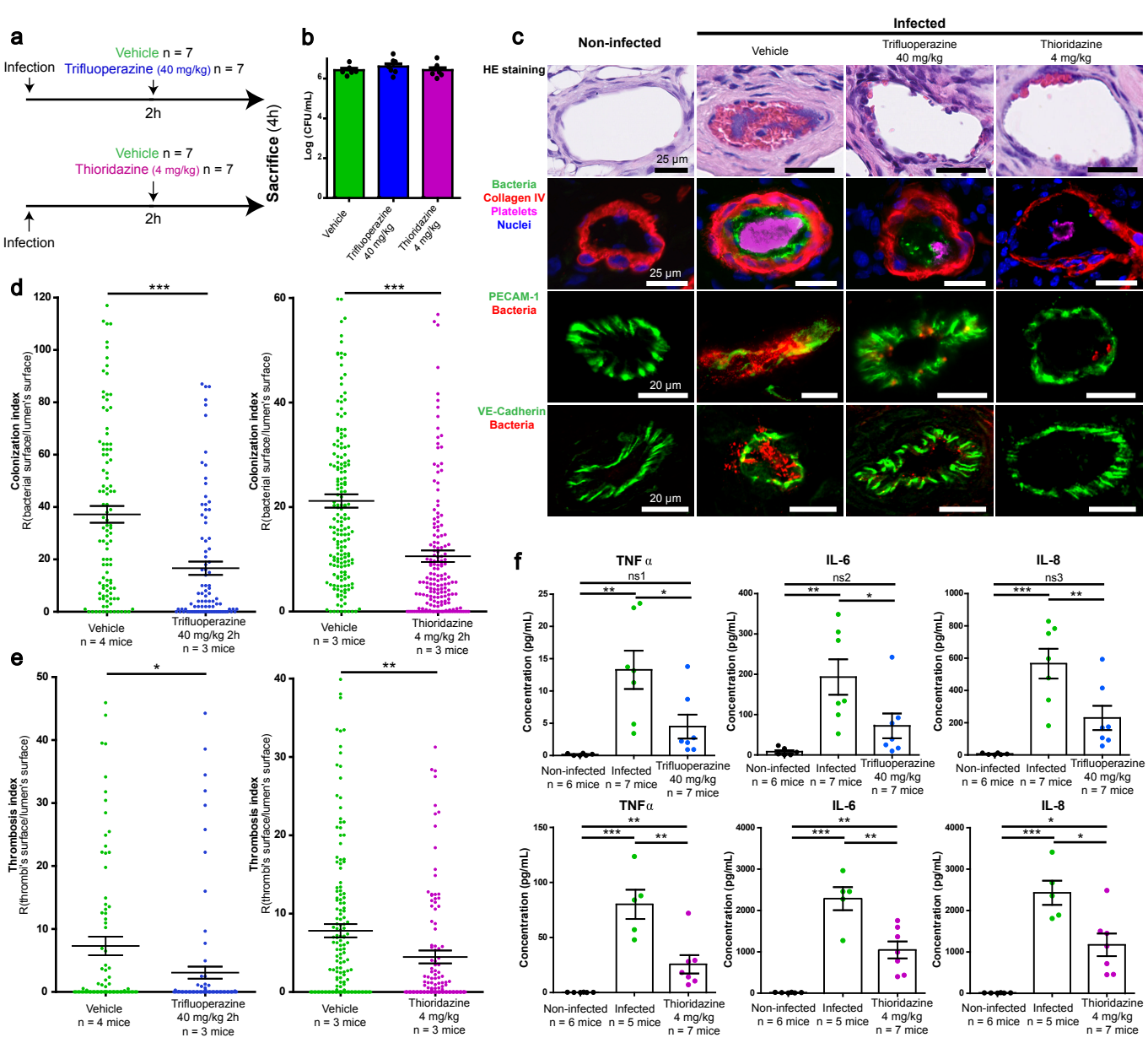
a
Infection
Vehicle n = 7
Trifluoperazine (40 mg/kg) n = 7
2h
Vehicle n = 7
Thioridazine (4 mg/kg) n = 7
2h
Infection
Sacrifice (4h)
b
Log (CFU/mL)
Vehicle
Trifluoperazine 40 mg/kg
Thioridazine 4 mg/kg
c
Non-infected
Infected
Vehicle
Trifluoperazine 40 mg/kg
Thioridazine 4 mg/kg
HE staining
Bacteria
Collagen IV
Platelets
Nuclei
PECAM-1
Bacteria
VE-Cadherin
Bacteria
25 µm
20 µm
d
Colonization index
R(bacterial surface/lumen's surface)
Vehicle n = 4 mice
Trifluoperazine 40 mg/kg 2h n = 3 mice
Vehicle n = 3 mice
Thioridazine 4 mg/kg 2h n = 3 mice
e
Thrombosis index
R(thrombi's surface/lumen's surface)
Vehicle n = 4 mice
Trifluoperazine 40 mg/kg 2h n = 3 mice
Vehicle n = 3 mice
Thioridazine 4 mg/kg n = 3 mice
f
TNF α
ns1
IL-6
ns2
IL-8
ns3
Concentration (pg/mL)
Non-infected n = 6 mice
Infected n = 7 mice
Trifluoperazine 40 mg/kg n = 7 mice
TNFα
IL-6
IL-8
Non-infected n = 6 mice
Infected n = 5 mice
Thioridazine 4 mg/kg n = 7 mice

Figure 5

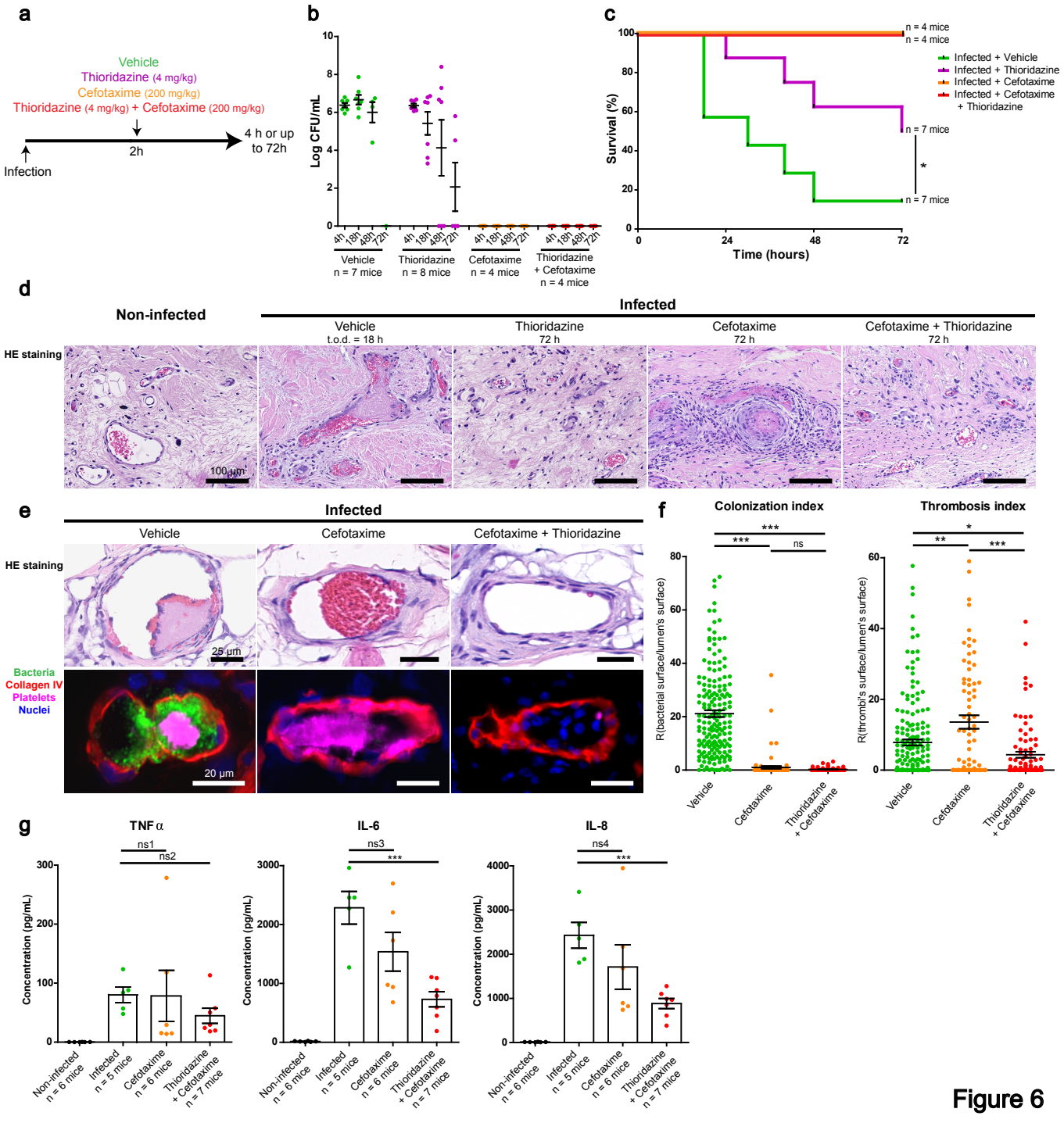
a
Vehicle
Thioridazine (4 mg/kg)
Cefotaxime (200 mg/kg)
Thioridazine (4 mg/kg) + Cefotaxime (200 mg/kg)
2h
4 h or up to 72h
Infection
b
Log CFU/mL
4h 18h 48h 72h
Vehicle n = 7 mice
Thioridazine n = 8 mice
Cefotaxime n = 4 mice
Thioridazine + Cefotaxime n = 4 mice
c
Survival (%)
Time (hours)
n = 4 mice
n = 4 mice
n = 7 mice
n = 7 mice
*
Infected + Vehicle
Infected + Thioridazine
Infected + Cefotaxime
Infected + Cefotaxime + Thioridazine
d
Non-infected
Infected
Vehicle t.o.d. = 18 h
Thioridazine 72 h
Cefotaxime 72 h
Cefotaxime + Thioridazine 72 h
HE staining
100 µm
e
Infected
Vehicle
Cefotaxime
Cefotaxime + Thioridazine
HE staining
25 µm
Bacteria
Collagen IV
Platelets
Nuclei
20 µm
f
Colonization index
Thrombosis index
R(bacterial surface/lumen's surface)
R(thrombi's surface/lumen's surface)
***
ns
*
**
Vehicle
Cefotaxime
Thioridazine + Cefotaxime
g
TNF α
IL-6
IL-8
Concentration (pg/mL)
ns1
ns2
ns3
ns4
Non-infected n = 6 mice
Infected n = 5 mice
Cefotaxime n = 6 mice
Thioridazine + Cefotaxime n = 7 mice

Figure 6